GaN-based Lamb-wave Mass-sensors on Silicon Substrates

Chi Ming Lee, Ka Ming Wong, Peng Chen and Kei May Lau
Electronic and Computer Engineering Department
Hong Kong University of Science and Technology (HKUST)
Clear Water Bay, Kowloon, Hong Kong
eekmlau@ust.hk

***Abstract*—Lamb-wave mass-sensors were fabricated with MOCVD-grown GaN-based thin films on silicon substrates. Crystalline GaN provides an alternative choice of material for fabricating Lamb-wave sensors. The advantageous properties of this material include high acoustic velocity, high chemical, mechanical and thermal stability, and the potential to integrate with a wide range of GaN-based devices such as high electron mobility transistor (HEMT) circuits, light emitting diodes (LED) and other photonic devices. We successfully developed GaN-based Lamb-wave mass-sensors in small size (membrane size of ~1mm × 1mm). The sensors showed good signal strength and mass sensitivity, comparable to other mass-sensors using conventional materials. This novel approach not only allows robust low-cost sensors to be fabricated, but also enables future integration with generic GaN-based devices on the same chip (i.e. lab-on-a-chip).**

I. INTRODUCTION

Acoustic wave sensors have numerous applications in chemical and biomolecular analysis [1], [2]. Lamb-wave sensors, and traditional surface acoustic wave (SAW) sensors and thickness shear mode (TSM) sensors (also known as quartz microbalance) are employed for such sensing applications. These three types of sensors are based on similar principle of piezoelectric effect for generation and transduction of acoustic waves, though the types of wave applied in each sensor are different. In addition, Lamb-wave-typed sensors differ from the other two types in the configuration of the electrodes and the thickness of the medium that acoustic waves propagate in. They are typically made of a thin propagation plate (~2-μm to 7-μm thick piezoelectric membrane) supported on a substrate, with electrodes in interlocking comb shape, also known as interdigitated transducers (IDTs) [2] – [8]. This configuration results in high mass sensitivity [2], [7], [9] and strong electromechanical coupling [10], thus making lamb-wave-typed sensors a competitive candidate for sensing applications. Among experimental results of reported lamb-wave sensors, almost all of them are based on sputtered piezoelectric materials, mostly aluminum nitride (AlN), zinc oxide (ZnO), and lead zirconate titanates (PZT) [2] – [9], [11].

We believe the choice of material for Lamb-wave sensors can be extended to crystalline gallium nitride (GaN), a piezoelectric material currently exploited in fabricating SAW radio frequency (RF) devices [14] and film bulk acoustic resonators (FBAR) [15]. The advantageous properties of this material include wide band gap (3.4eV), high chemical, mechanical and thermal stability, high acoustic velocity [12], and the potential to integrate with a wide range of GaN-based devices such as high electron mobility transistor (HEMT) circuits, light emitting diodes (LED) and other photonic devices. Recently, the maturity of metalorganic chemical vapor deposition (MOCVD) technology allows versatile sensors to be fabricated with high-quality epitaxial GaN on (111) silicon (Si) substrates instead of on sapphire and silicon carbide (SiC) substrates, whilst conventional Si-based semiconductor processing techniques can still be adopted.

In this study, we developed small-sized GaN-based mass-sensors operating in high-frequency lowest order symmetric (S_0) Lamb-wave mode on silicon substrates. There are a number of advantages. Firstly, the epitaxial GaN-based thin layers used as sensors are the optimized result of strain engineering with the aim of combining low cost and reliability. Secondly, the small size of sensors (i.e. ~1 mm × 1 mm area of the sensing membrane in our case, in comparison with common centimeter scale Lamb-wave sensors [2] – [4], [6], [9]) can improve mechanical robustness and fabrication yield, as well as conservation of costly reagents and analytical throughput in diagnostic applications (more sensing elements encompassed in each microarray). Thirdly, the high operating frequency resulting from the high phase velocity of the S_0 Lamb-wave, as compared with SAW and lowest order anti-symmetric (A_0) Lamb-wave [4], [9], can enhance sensitivity of this type of sensors.

II. SENSOR DESIGN & STRUCTURE

Fig. 1a shows a schematic of the sensor structure. After removal of the silicon substrate at the center, the ~1-μm piezoelectric sensing membrane suspends in air. The two chromium/gold IDTs were placed on the suspended membrane close to the left/right edges of the backside cavity of the substrate and electrically connected to the RF probe contact

pads, as shown in the optical micrograph of the sensor (Fig. 1b). The design parameters of the IDTs are listed in Table I.

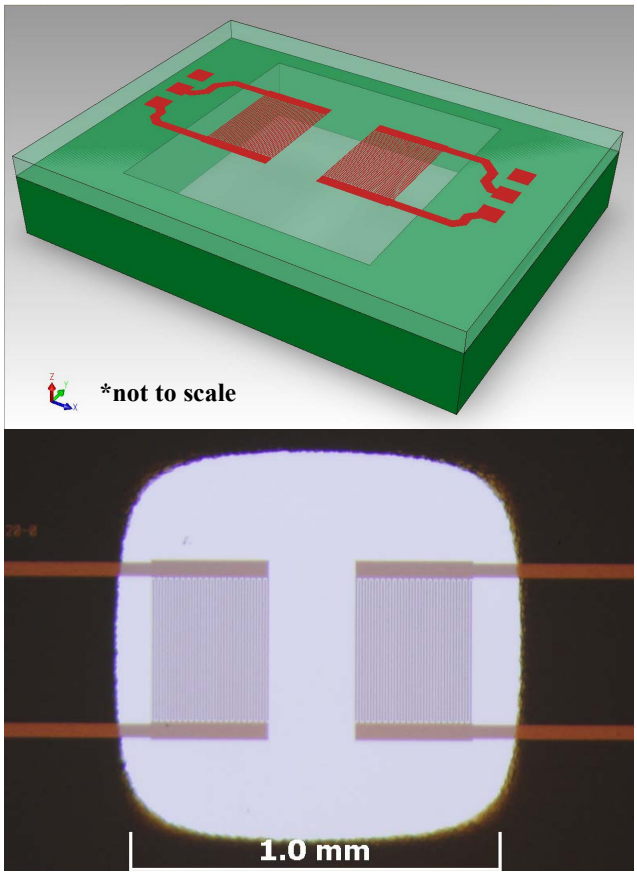

Figure 1: (a) (top) the schematic of the sensor structure. (b) (bottom) the top view of the transparent membrane of the sensor under microscope.

TABLE I.

Design Parameters of IDTs and membrane	
Acoustic Wavelength	16 μm
Number of pairs of each IDT	15
IDT Aperture	400 μm
IDT Separation (center to center)	480 μm
Total thickness of the membrane	1.085 μm

III. FABRICATION

There are four main processing steps in the fabrication of the sensors, with schematics shown in Fig. 2. To minimize noise due to electromagnetic feedthrough, high-resistivity silicon substrates were used [13].

A. MOCVD of GaN-based thin films on Si Substrates

A stack of GaN-based epitaxial layers were grown on a high-resistivity silicon (111) substrate by MOCVD, as illustrated in Fig. 2a.

B. Fabrication of IDT Electrodes on Top-Side

Chromium/gold (3 nm / 30 nm) IDT electrodes were fabricated by the lift-off process on top of the epi-layers. The IDT electrode patterns were defined by photolithography on the front side with regular photoresist, followed by metal deposition using an e-beam metal evaporation system and then lift-off.

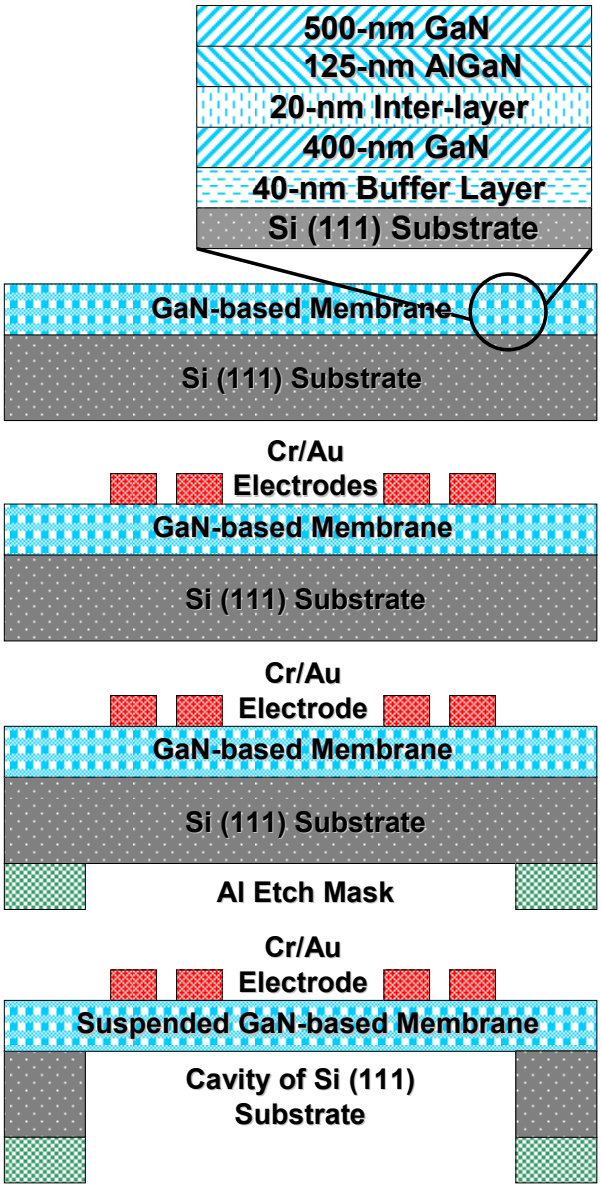

Figure 2. The process flow for fabricating the sensor. (diagrams from top to bottom) (a) MOCVD of GaN-based thin films on Si Substrates. Inset: the magnified diagram that shows the material structure of the GaN-based membrane (b) Fabrication of IDT Electrodes on Top-Side. (c) Patterning Etch Mask on Backside. (d) Silicon Dry Etching on Backside.

C. Patterning Etch Mask on Backside

Similar photolithography techniques as in step B were employed to pattern a 300-nm thick Al etch mask on the backside of the Si substrate to create an 1-mm square-shaped opening for substrate removal.

D. *Silicon Dry Etching on Backside*

Release of the suspended membrane was accomplished by inductively coupled plasma (ICP) etching on the backside of the Si substrate with a SF_6-based gas. The silicon etching was selective to gallium nitride.

IV. MEASUREMENT RESULTS

Characteristics of unloaded sensors were evaluated with a network analyzer after fabrication. The insertion loss and the phase, of the S_{21} parameter versus frequency were measured. The point of maximum signal strength (minimum insertion loss) was observed at 471.3MHz with a magnitude of ~ −29 dB, corresponding to the S_0 Lamb wave, as illustrated in Fig. 3. The corresponding phase velocity is ~7540m/s for the 16-μm wavelength and 1.1-μm total thickness of GaN-based thin films, in good agreement with a recent publication [12].

The mass sensitivity of the sensors was then evaluated by loading/depositing different thicknesses of silicon oxide (SiOx) on the backside of the membranes using plasma-enhanced chemical vapor deposition (PECVD). The characteristic changes of the S_{21} parameters (due to mass-loading effect in acoustic wave propagation path) were recorded. A tabletop film analysis system, Nanometrics NanoSpec 3000, was used to measure the thicknesses of the deposited SiO_2. A linear relationship between the frequency/phase shift and thicknesses of deposited SiO2 was derived, as shown in Fig 4. By normalizing the gradient of the linear fits in unit mass per area, the mass sensitivities in terms of frequency shift (in parenthesis: sensitivity normalized by the frequency in unloaded state), and that of phase shift at 471.3MHz were further derived to be −82GHz / (g·cm^{-2}) (or −174 cm^2/g) and −3.09×10^6 deg / (g·cm^{-2}), respectively. Comparable results can be found in previous larger sensors using other piezoelectric materials and structures [2], [4], [7].

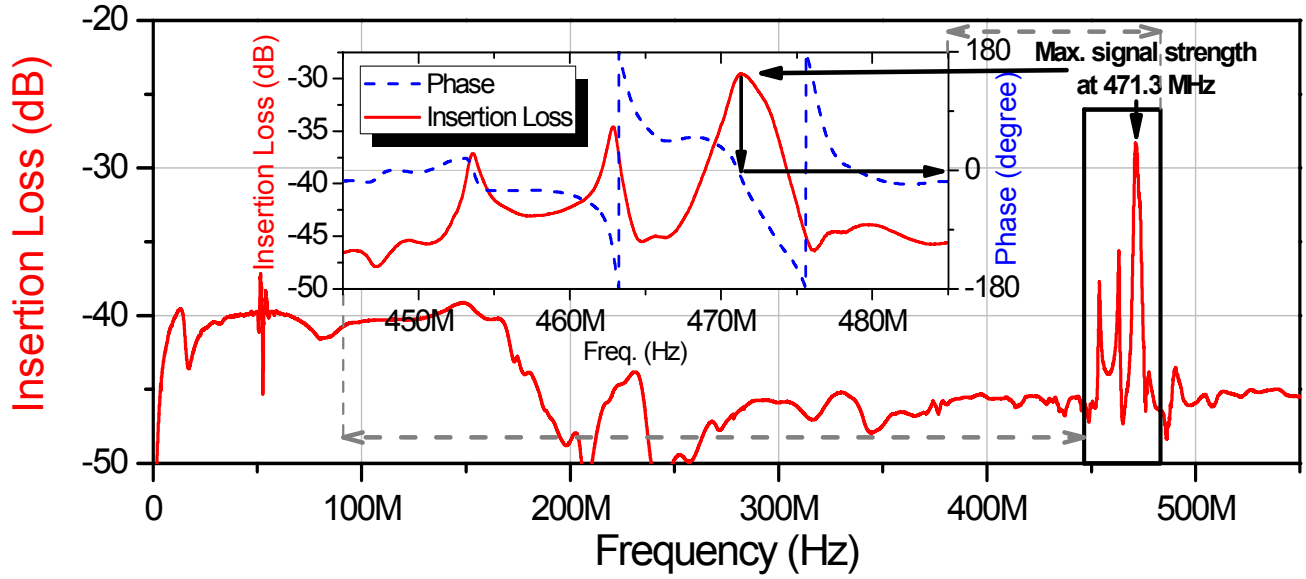

Figure 3. The insertion loss of S21 parameter of the sensor versus frequency. Inset: The magnified diagram that shows the S_{21} insertion loss and phase in unload state.

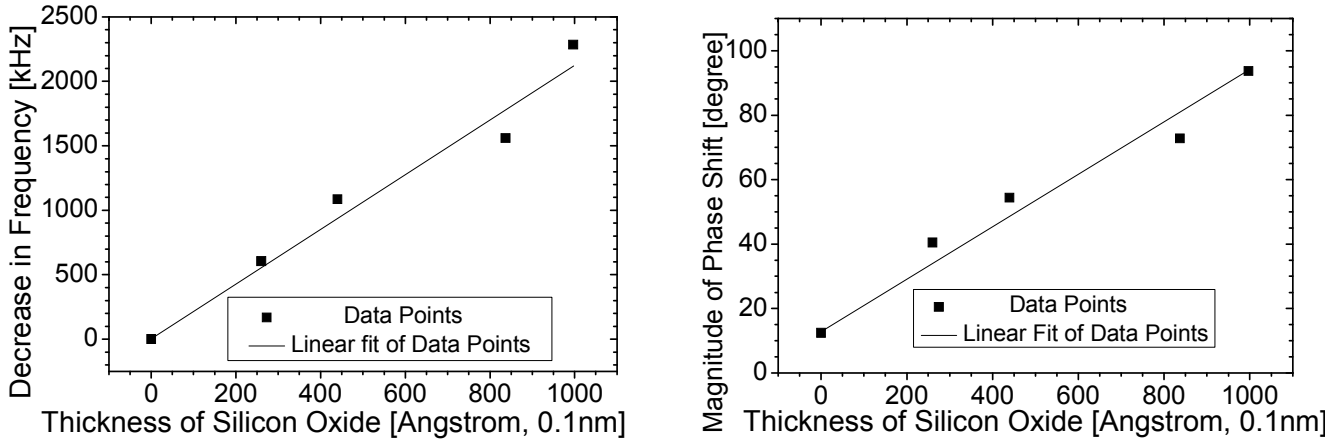

Figure 4. The plots of the signal response against different thicknesses of silicon oxide. (a)(left) The frequency shift of the peak of maximum signal strength (mininum insertion loss). (b)(right) The magnitude of phase shift at the frequency of the original peak with no silicon oxide deposited (i.e. 471.3 MHz)

V. CONCLUSION

Small-sized Lamb-wave mass-sensors based on crystalline GaN thin films on silicon substrates were developed and evaluated. This novel approach demonstrates the potential of fabricating generic GaN-based devices on a single chip (i.e. lab-on-a-chip). Further research and development can be performed on the synergy of local and global integration of GaN-based devices and micro-electro-mechanical systems (MEMS) on a silicon platform.

ACKNOWLEDGMENT

This work was supported by a grant (CA07/08.EG02) from the Research Grants Council. Support of the Nanofabrication Facilities (NFF) of HKUST is also acknowledged.

REFERENCES

[1] K. Lange, B. E. Rapp, M. Rapp, "Surface acoustic wave biosensors: a review," Analytical and Bioanalytical Chemistry, 391 (5), pp. 1509-1519, 2008.

[2] D. S. Ballantine, R. M. White, S. J. Martin, A. J. Ricco, G. C. Frye, E. T. Zellers, and E. T. Wohltjen, "Acoustic wave sensors: theory, design and physico-chemical applications," Academic, New York, 1997.

[3] W.-Y. Chang, P.-H. Sung, C.-H. Chu, C.-J. Shih, and Y.-C. Lin, "Phase detection of the two-port FPW sensor for biosensing," IEEE Sensors Journal, Vol. 8, No.5, pp. 501-507, May 2008.

[4] S. W. Wenzel, and R. M. White, "A multisensor employing an ultrasonic Lamb-wave Oscillator," IEEE Transactions on Electron Devices, Vol. 35, No. 6, June 1988.

[5] R. Hino, M. Esashi, and S. Tanaka, "Antisymmetric-mode Lamb wave methanol sensor with edge reflectors for fuel cell applications," Proceedings of the IEEE International Conference on Micro Electro Mechanical Systems (MEMS), art. no. 5442345, pp. 871-874, 2010.

[6] I.-Y. Huang, and M.-C. Lee, "Development of a FPW allergy biosensor for human IgE detection by MEMS and cystamine-based SAM technologies," Sensors and Actuators, B: Chemical 132 (1), pp. 340-348, 2008.

[7] R. Duhamel, L. Robert, H. Jia, F. Li, F. Lardet-Vieudrin, J.-F. Manceau, and F. Bastien, "Sensitivity of a Lamb wave sensor with 2 μm AlN membrane," Ultrasonics 44 (SUPPL.), pp. e893-e897, 2006.

[8] J. Pepper, R. Noring, M. Klempner, B. Cunningham, A. Petrovich, R. Bousquet, C. Clapp, J. Brady, and B. Hugh, "Detection of proteins and intact microorganisms using microfabricated flexural plate silicon resonator arrays," Sensors and Actuators, B: Chemical 96 (3), pp. 565-575, 2003.

[9] T. Laurent, F. O. Bastien, J.-C. Pommier, A. Cachard, D. Remiens, and E. Cattan, " Lamb wave and plate mode in ZnO/silicon and AlN/silicon membrane – Applications to sensors able to operate in contact with liquid," Sensors and Actuators, A: Physical 87 (1-2), pp. 26-37, 2000.

[10] E. L. Adler, "Electromechanical Coupling to Lamb and Shear-Horizontal modes in piezoelectric plates," IEEE Transactions on Ultrasonics, Ferroelectrics, and Frequency Control, Vol. 36, No. 2, pp. 223-230, March 1989.

[11] Y. S. Lee, D. S. Yoon, and T. S. Kim, "Improvement of the mass sensitivity in flexural plate wave biosensor based on PZT thin film," Integrated Ferroelectrics 69, pp. 391-400, 2005.

[12] A. K. Pantazis, E. Gizeli, and G. Konstantinidis, "A high frequency GaN Lamb-wave sensor device," Applied Physics Letters 96 (19), art. no. 194103, 2010.

[13] J. H. Visser, and A. Venema, "Silicon SAW devices and electromagnetic feedthrough," Ultrasonics Symposium Proceedings 1, pp. 297-301, 1988.

[14] T. Lalinsky, L. Rufer, G. Vanko. S. Mir, S. Hascik, Z. Mozolova, A. Vincze, and F. Uherek, "AlGaN/GaN heterostructure-based surface acoustic wave-structures for chemical sensors," Applied Surface Science 255, pp. 712-714, 2008.

[15] D. Neculoiu, G. Konstantinidis, A. Muller, A. Kostopoulos, D. Vasilache, K. Mutamba, C. Sydlo, H. L. Hartnagel, L. Bary, and R. Plana, "Microwave FBAR structures fabricated using micromachined GaN membranes," IEEE MTT-S International Microwave Symposium Digest , art. no. 4263961, pp. 877-880, 2007.